

Monitoring Breast Cancer Response to Neoadjuvant Chemotherapy Using Ultrasound Strain Elastography

FERNANDES, J., SANNACHI, L., TRAN, William, KOVEN, A., WATKINS, E., HADIZAD, F., GANDHI, S., WRIGHT, F., CURPEN, B., EL KAFFAS, A., FALTYN, J., SADEGHI-NAINI, A. and CZARNOTA, G.

Available from Sheffield Hallam University Research Archive (SHURA) at:

<https://shura.shu.ac.uk/25875/>

This document is the Published Version [VoR]

Citation:

FERNANDES, J., SANNACHI, L., TRAN, William, KOVEN, A., WATKINS, E., HADIZAD, F., GANDHI, S., WRIGHT, F., CURPEN, B., EL KAFFAS, A., FALTYN, J., SADEGHI-NAINI, A. and CZARNOTA, G. (2019). Monitoring Breast Cancer Response to Neoadjuvant Chemotherapy Using Ultrasound Strain Elastography. *Translational Oncology*, 12 (9), 1177-1184. [Article]

Copyright and re-use policy

See <http://shura.shu.ac.uk/information.html>

Monitoring Breast Cancer Response to Neoadjuvant Chemotherapy Using Ultrasound Strain Elastography



Jason Fernandes^{*}, Lakshmanan Sannachi^{*††}, William T. Tran^{*†,‡,‡‡}, Alexander Koven^{*}, Elyse Watkins^{*}, Farnoosh Hadizad^{*}, Sonal Gandhi[¶], Frances Wright[#], Belinda Curpen^{**}, Ahmed El Kaffas^{††}, Joanna Faltyn^{††}, Ali Sadeghi-Naini^{*,†,**,††} and Gregory Czarnota^{*,†,§,**,††}

^{*}Department of Radiation Oncology, Sunnybrook Health Sciences Centre, Toronto, CA; [†]Department of Radiation Oncology, University of Toronto, Toronto, CA; [‡]Centre for Health and Social Care Research, Sheffield Hallam University, Sheffield, UK; [§]Department of Medical Biophysics, University of Toronto, Toronto, CA; [¶]Division of Medical Oncology, Sunnybrook Health Sciences Centre, Toronto, CA; [#]Division of Surgical Oncology, Sunnybrook Health Sciences Centre, Toronto, CA; ^{**}Department of Medical Imaging, Sunnybrook Health Sciences Centre, Toronto, CA; ^{††}Physical Sciences, Sunnybrook Research Institute, Toronto, CA; ^{‡‡}Institute of Clinical Evaluative Sciences, Sunnybrook Research Institute, Toronto, CA

Abstract

Strain elastography was used to monitor response to neoadjuvant chemotherapy (NAC) in 92 patients with biopsy-proven, locally advanced breast cancer. Strain elastography data were collected before, during, and after NAC. Relative changes in tumor strain ratio (SR) were calculated over time, and responder status was classified according to tumor size changes. Statistical analyses determined the significance of changes in SR over time and between response groups. Machine learning techniques, such as a naïve Bayes classifier, were used to evaluate the performance of the SR as a marker for Miller-Payne pathological endpoints. With pathological complete response (pCR) as an endpoint, a significant difference ($P < .01$) in the SR was observed between response groups as early as 2 weeks into NAC. Naïve Bayes classifiers predicted pCR with a sensitivity of 84%, specificity of 85%, and area under the curve of 81% at the preoperative scan. This study demonstrates that strain elastography may be predictive of NAC response in locally advanced breast cancer as early as 2 weeks into treatment, with high sensitivity and specificity, granting it the potential to be used for active monitoring of tumor response to chemotherapy.

Translational Oncology (2019) 12, 1177–1184

Introduction

According to the Canadian Cancer Society, an estimated 99,500 women in Canada were diagnosed with cancer in 2016, with 26% of these cases being breast cancers. Breast cancer is the most common cancer type diagnosed in females, with 1 in 9 Canadian females estimated to receive a diagnosis in their lifetime [1]. Approximately 10% of breast cancer cases diagnosed in Canada will be locally advanced breast cancers (LABCs) [2]. LABC refers to the most advanced breast tumors with the absence of any distant metastases [3]. Although the exact definition of LABC tends to vary across the

Address all correspondence to: Dr. Gregory J. Czarnota, MD, PhD, Department of Radiation Oncology, 2075 Bayview Avenue, T2, Toronto, Ontario, Canada M4N3M5. E-mail: gregory.czarnota@sunnybrook.ca;

Received 13 December 2018; Revised 3 May 2019; Accepted 6 May 2019

© 2019 The Authors. Published by Elsevier Inc. on behalf of Neoplasia Press, Inc. This is an open access article under the CC BY-NC-ND license (<http://creativecommons.org/licenses/by-nc-nd/4.0/>).

1936-5233/19

<https://doi.org/10.1016/j.tranon.2019.05.004>

literature, the U.S. National Comprehensive Cancer Network defines it as a tumor greater than 5 cm with regional lymphadenopathy, a tumor which involves the skin or chest wall regardless of size or nodal status, or the presence of regional lymphadenopathy irrespective of tumor stage [4]. LABC is typically inoperable and, despite aggressive treatment, is associated with poorer prognosis than earlier-stage breast cancer due to eventual metastasis [5].

The current recommended standard of care for LABC includes neoadjuvant chemotherapy (NAC), usually followed by modified radical mastectomy, and then radiation therapy. When first-line neoadjuvant chemotherapy fails to achieve a suitable response, other treatments must be considered, such as second-line therapy, hormonal therapy, or immediate surgery [6]. The ideal outcome of neoadjuvant treatment, however, is pathological complete response (pCR), in which there is no residual invasive tumor or node metastases, although *in situ* carcinoma may still be present [7]. The evaluation of pCR after neoadjuvant therapy is associated with better rates of long-term survival in breast cancer [8]. Additionally, pCR or sufficient downstaging in response to NAC may allow breast-conserving surgery to be used as an alternative to radical mastectomy as part of the treatment regimen [9]. Knowledge of how a tumor is responding to treatment is essential to guiding further treatment options. When tumor response is ideal, more conservative treatment options may be explored, as in the case of opting for breast-conserving surgery over radical mastectomy. Conversely, when a tumor fails to respond to NAC, early knowledge of this could be used to halt ineffective chemotherapy so that new chemotherapeutic options may be pursued and better tumor response may be achieved prior to surgery. Currently, the response to NAC is determined pathologically at the time of surgery. Consequently, NAC may be optimized by finding a modality which can gauge treatment response during NAC rather than following its completion.

Current methods of monitoring tumor response to NAC include MRI and ¹⁸F-FDG PET/CT [10–13]. Sonography, mammography, and palpation have also been used to measure response to neoadjuvant therapy with a lesser degree of success [14]. This study evaluated compression elastography as a means of monitoring tumor response to NAC. Previous studies have indicated that there is a correlation between changes in tumor mechanical parameters and a favorable response to NAC [15]. Compression elastography measures deformations in a tissue in response to a static compression applied by the sonographer through the ultrasound transducer [16]. Within a region of interest (ROI), the tissue strain (ϵ), which is the change in length per unit length of tissue, can be quantified by measuring the tissue displacement across multiple frames after a stress has been applied by the operator [16,17]. Assuming the stress (σ) being applied by the operator is constant across all scans, Hooke's law ($\sigma = E\epsilon$) can be used to derive Young's modulus (E) (i.e., elastic modulus) of tissue. Young's modulus is representative of the tissue's elasticity and its ability to resist deformation in the presence of stress.

Ultrasound imaging has the advantage of being portable, accessible, and inexpensive. Elastography has already been evaluated in terms of its ability to detect prostatic, breast, and thyroid lesions [18–20]; as well as having utility in nononcologic practice. Shear-wave elastography, another ultrasound-based modality, also seeks to determine a tissue's stiffness. The difference is that it uses acoustic radiation force to introduce a disturbance as opposed to manual compression, and measures the speed of propagation of shear waves as opposed to the degree of tissue deformation [21]. Both methods have demonstrated comparable performance in improving the diagnostic abilities of B-

mode ultrasound [21]. Monitoring response to neoadjuvant chemotherapy using elastography would prove less expensive and be more available than the current standards of MRI and PET/CT.

Here, we investigate the use of ultrasound elastography to monitor NAC-induced changes in tumor stiffness. The study objective was to differentiate between pathological complete responders (pCRs) and nonpathologic complete responders (npCRs) within a sample of 92 LABC patients. We collected compression ultrasound data prior to the start of NAC treatment and at multiple times throughout the treatment leading up to surgery. A comparison of the elastography results with pathology acquired postoperatively indicates that the strain ratio (SR), as calculated in this study, can differentiate responders from nonresponders.

Materials and Methods

Patients and Treatment

This study was approved by the institution's research ethics board. Participants were informed of the study details prior to signing a

Table 1. Patient Clinical Information.

Patient and Tumor Characteristics	p C R (n = 21)	N o n - p C R (n = 71)
Age (median, years)	55	50
Sex	Male Female	1 70
Menopause status	Premenopausal Postmenopausal Perimenopausal N/A	5 26 2 4
Pretreatment tumor size (largest diameter, cm)	3.53 ± 1.75	5.46 ± 2.53
Posttreatment tumor size (largest diameter, cm)	N/A	2.97 ± 3.18
Molecular subtype	Luminal (10%) Basal-like HER-2 positive	9 14 (15%) 5 (5%)
Stage		
Primary tumor (T)	T1 T2 T3 T4 T4b T4d Unavailable	1 (1%) 21 (23%) 20 (22%) 1 (1%) 1 (1%) 2 (2%) 25 (27%)
Node involvement (N)	N0 N1 (10%) N2 N3 Unavailable	13 (14%) 29 (32%) 3 (3%) 0 26 (28%)
Chemotherapy regimen		
FEC-D (fluorouracil, epirubicin and cyclophosphamide followed by docetaxel)	6 (7%)	33 (36%)
AC-T (doxorubicin (Adriamycin) and cyclophosphamide followed by paclitaxel (Taxol))	1 (1%)	34 (37%)
TC (paclitaxel (Taxol) and cyclophosphamide)	1 (1%)	4 (4%)
AC (doxorubicin (Adriamycin) and cyclophosphamide)	1 (1%)	0
AC-D (doxorubicin (Adriamycin) and cyclophosphamide followed by docetaxel)	1 (1%)	0
Carboplatin and paclitaxel (Taxol) followed by doxorubicin (Adriamycin) and cyclophosphamide	1 (1%)	0

Patient demographics, tumor characteristics, and treatment details prior to and after NAC. Patients, whose data are presented in this table, were not consecutively recruited.

written consent. Ninety-two (92) patients with biopsy-confirmed LABC were enrolled in this study. Of the 92 LABC patients, 61 patients had luminal breast cancer, 21 had basal-like breast cancer, and 10 had human epithelial growth factor receptor-2 positive (HER2+) type breast cancer. Twenty-one patients exhibited a pCR and 71 exhibited npCR. As part of the patients' usual care, pretreatment assessment involved a physical examination, breast imaging (x-ray mammography and conventional ultrasound), and tissue biopsy for diagnostic workup. All participants were given standard treatment as per institutional guidelines. Patients received NAC, consisting of a combination of anthracycline and taxane-based drugs, spanning over approximately 18 weeks (Table 1). Patients who tested HER2+ received trastuzumab during taxane chemotherapy. Following NAC, patients underwent a radical mastectomy and pathological assessment.

Assessment of Tumor Response

As part of the patients' usual standard of care, a board-certified breast pathologist examined slide-mounted mastectomy specimens, which were stained using hematoxylin and eosin. For the study here, tumor characteristics, such as tumor size, histologic subtype, and molecular features [estrogen receptor (ER), or HER2], were reported. Specimens were examined microscopically for pathological response, and this was in accordance with institutional guidelines. Results of the pathological response were recorded in the patient's medical record. Patients were classified using modified-RECIST criteria based on tumor size change [22]. Briefly, these criteria were categorically scaled between an RS (response score) of 1-5, where RS1 demonstrates no change or reduction in size, RS2 indicates minor reductions in size (up to 30%), RS3 demonstrates 30%-90% reduction in tumor size, RS4 indicates significant reduction in tumor size (more than 90% size reduction, though not a complete response), and RS5 indicates a complete absence of invasive tumor on imaging and confirmed via pathological examination. This incorporated standard, size-based reporting but in addition allowed the discernment of patients with a subjectively very good response from those with a complete response. For statistical purposes of the receiver operating characteristic (ROC) curve, patients were categorized as either pathologically complete responders (RS5) or non-pathologically complete responders (RS1-4). Nodal response was not included in the analysis which focused on primary tumor response only.

Imaging Study

Ultrasound elastography data were collected prior to the start of chemotherapy (baseline), during treatment (weeks 1, 4, 8, and 12, relative to the start of NAC), and a final scan 1 week prior to surgery (preop). A Sonix RP system (Ultrasonix, Vancouver, Canada) with an L14-5, 60-mm transducer was used to collect brightness-mode (B-mode) images and elastography data (at a nominal center-frequency of 7 MHz). All imaging data in this study were collected by the same research sonographer. The sonographer followed standardized imaging protocols and maintained a consistent compression force during the scan series. To ensure consistency between imaging time points, the position and direction of the ultrasound transducer were noted in the patient's clinical notes at the first imaging session and replicated at each subsequent session. Strain data were collected using quasistatic compressions onto the breast to measure the relative tissue distortions. The compression applied onto the subject's breast was adjusted with reference to a built-in indicator on the ultrasound device that estimates the applied deformation [23]. Static scans were

acquired at three fixed points that sampled tumor tissue and two additional points within the adjacent fatty breast tissue (nonmalignant) as controls. The focal depth ($f_d = 1.75$ cm) and scan size were kept constant (lateral length = 6 cm, axial length = 4 cm) during the imaging series. Empirical strain values were captured digitally and displayed on a 256-color map scale. Ultrasound B-mode images were co-registered to the elastography color maps to guide tumor segmentation.

Elastography Analysis

Strain images were generated by the Ultrasonix native motion estimation algorithm. This method relies on a one-dimensional, normalized, cross-correlation where the shift in the peak of the cross-correlation curve is used to estimate tissue deformation [24,25]. The estimated strain values were further analyzed offline using a C++-based software (Evrika Research Technologies, Toronto, Canada) to calculate tissue SRs based on the Ultrasonix elastography data. A breast radiologist was consulted for tumor segmentation based on the B-mode images obtained within each scan.

For analysis, ROIs were selected from the tumor and the surrounding normal breast tissue on B-mode images. A dynamic ROI corresponding to the tumor was identified using a low-pass filtered threshold to detect the tumor edge in the pretreatment scan. These ROIs were then adjusted for subsequent scans based on the shape and size of the tumor. Next, B-mode ROIs were co-registered with the strain maps. Finally, the mean strain values within the tumor ROIs and normal breast tissue ROIs were calculated (Figure 1). SRs were calculated by dividing the mean strain measured in an ROI contained within normal breast tissue by the mean strain measured in an ROI contained within tumor tissue as in Eq. [1] [26,27] below.

$$SR = \frac{\text{Mean strain}_{\text{Breast normal tissue ROI, } d_x(\text{cm})}}{\text{Mean strain}_{\text{Tumor ROI, } d_x(\text{cm})}} \quad (1)$$

where $d_x(\text{cm})$ represents ROIs selected at equal depths within the tissue. The mean SRs were calculated over the whole tumor, and changes over time were computed as percentage decrease (%) relative to the baseline.

Statistical Analysis

Statistical analysis was conducted to test for significance in measured changes in strain parameters (strain) over time using a repeated-measures ANOVA (95% CI, $\alpha = 0.05$). Additionally, pCR and npCR groups were compared for statistically significant differences in SR% decrease at each time period using independent t tests. Differences were considered significant at an alpha level of 0.05 or less ($P < .05$). Further analysis comparing responders to nonresponders was also performed using alternative definitions of response (RS4-5 and RS3-5). Finally, ROC analysis (SPSS, Chicago, IL) was carried out to estimate the sensitivity and specificity using the Q index — the point on the ROC where the sensitivity and the specificity are equal. This was only done on the groups using the pathologically complete definition of response (RS5). In order to predict tumor response, classification analyses were performed on estimated SR parameters using naive Bayes and k-nearest neighbor (k-NN) classifiers. A naive Bayes classification algorithm assumes that the features are independent of each other within the class. The k-NN classifier classifies a test sample based on frequency and distance to k-nearest training samples. In this study, the class imbalance problem was circumvented by subsampling the original data sets into 20

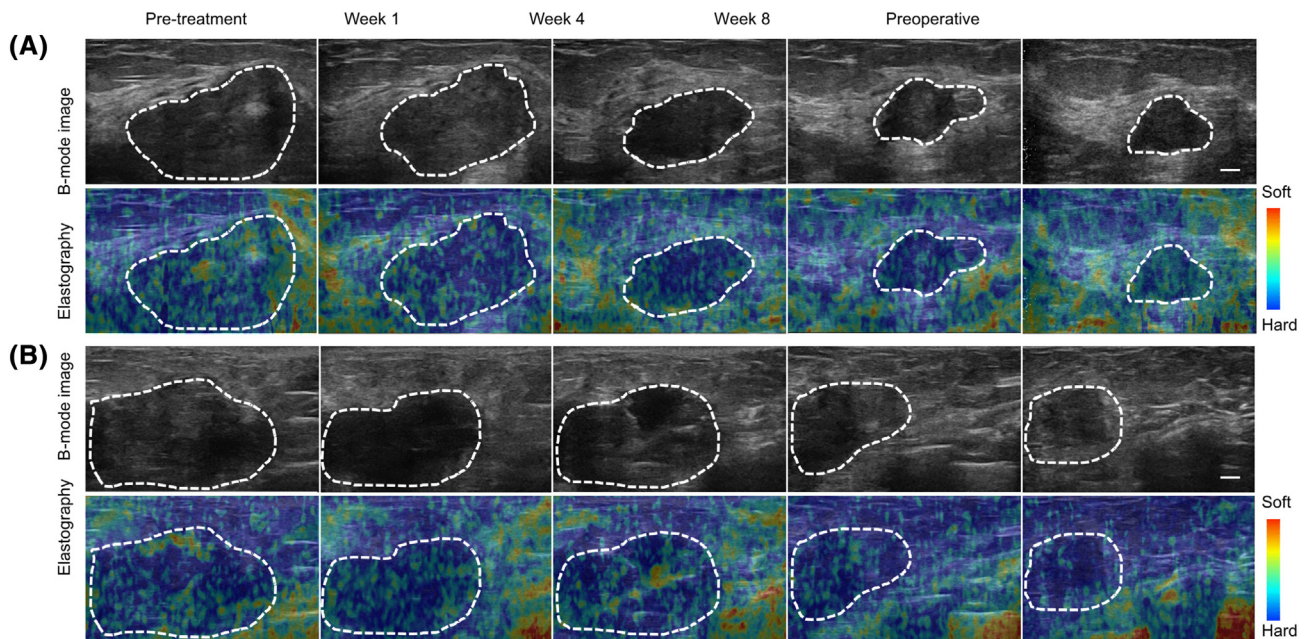


Figure 1. Representative B-mode and elastography images acquired during and after completion of chemotherapy. (A) Representative ultrasound B-mode and elastography images from a pCR patient's tumor taken at baseline; weeks 1, 4, and 8; and after completion of chemotherapy (preop). The responding patient demonstrated progressive changes in both tumor morphology and tumor strain. (B) Representative ultrasound B-mode and elastography images from an npCR patient's tumor taken at baseline; weeks 1, 4, and 8; and after completion of chemotherapy (preop). SR changed significantly for the nonresponder over the course of treatment, however, to a lesser degree than the change seen with the pCR patient. Static (fixed-sized) ROIs were used in selecting the tumor region to estimate strain values for each patient. Scale bar = 1 cm, color bar = hard (blue) to soft (red) (0 to 255).

subsets such that each subset had an equal number of pCR and npCR, and also all patients in the classes were selected at least once over all subsets. Sensitivity, specificity, accuracy, and area under the curve (AUC) were calculated to determine the performance of the classification, and the results were validated using leave-one-out cross-validation. A subanalysis was conducted as well using patients with luminal (ER+/PR+/HER-2 \pm), basal (ER-/PR-/HER-2-), and HER-2-enriched (ER-/PR-/HER-2+) molecular subtypes.

Results

The study included 21 pCRs and 71 npCRs. All patients received chemotherapy. Details of the treatment regimens are provided in Table 1. The majority of patients received anthracycline and taxane-based treatments. Representative B-mode and elastography images are presented in Figure 1 for a pCR (Figure 1A) and an npCR (Figure 1B). These demonstrated clearly definable hypoechoic breast cancer masses. Elastographic images were noisy and typical of other studies on patients with locally advanced breast cancer [23].

Figure 2 presents the results of a quantitative analysis of the changes in SR for all patients ($n = 92$) with different treatment times and using different associations of response scores as “responders” and “nonresponders.” Changes between responders and nonresponders began early on after the administration of chemotherapy. The magnitude of difference between responder and nonresponder classes was dependent on the response definitions used (pCR versus npCR, RS score). The SRs obtained from the elastography data were compared using the relative change of the SR, at a given time, compared to the baseline values. As indicated in Figure 2A, both the pCR and npCR outcome groups exhibited a significant decrease in SR over the course of treatment ($P < .001$ for both) by week 4.

Significance testing was conducted to compare the pCR and npCR groups. Significant differences in the change from the baseline value appeared by the second week of treatment ($P < .05$). By the second week of treatment (Table 2), the pCR outcome group had already experienced a $12\% \pm 13\%$ decrease in SR, whereas the non-pCR outcome group had only experienced a $3\% \pm 11\%$ decrease (Table 2). The decrease from baseline continued to increase in magnitude with continued cycles of chemotherapy. By weeks 8 and 12, the pCR group experienced a $25\% \pm 16\%$ and $30\% \pm 17\%$ decrease from baseline, respectively, whereas the npCR group only experienced a $16\% \pm 11\%$ and $17\% \pm 13\%$ decrease at the same time periods, respectively (Table 2). These results suggest that tumors that maintain a consistent SR and remain stiff over the course of NAC are less likely to achieve a pathologically complete response. Supplementary Figure 1 presents the results of a subgroup analysis based on molecular subtypes of the LABC tumors. Corresponding values, statistical measures, and results are found in Supplementary Table 1.

The results of ROC analysis comparing pCR to npCR are presented in Table 3. Results indicate the sensitivity (%Sn), specificity (%Sp), and AUC that were produced using naïve Bayes or k-NN classifiers. Data analysis was performed using the difference in SR from baseline at weeks 1, 4, and 8 and preoperatively. Following 1 week of treatment, classification was poor with a %Sn/%Sp/AUC of 80%/64%/64%. However, by week 4, this improved to 86%/83%/75%. The %Sn/%Sp/AUC further improved to 87%/80%/77% by week 8 and were the most adequate predictors of pathological response preoperatively with %Sn and %Sp of 84% and 85%, respectively, and an AUC of 81% (Table 3).

The same statistical analysis used to compare pCR to npCR was also performed to compare alternative definitions of response,

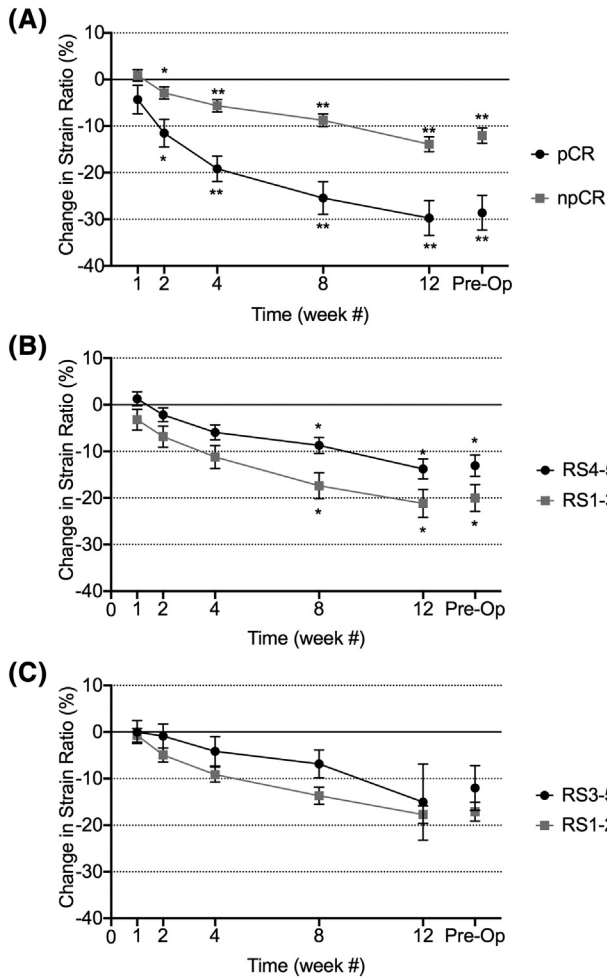


Figure 2. Changes in SR, as monitored during and at the completion of neoadjuvant chemotherapy. (A) SRs for pathologically complete responders (RS5) and non-pathologically complete responders (RS1-4). Corresponding representative mastectomies (not shown) of responders and nonresponders demonstrate differences in the overall tumor morphology between response groups. (B) SRs for tumors with response scores 4-5, representing responders, and response scores 1-3, representing nonresponders. (C) SRs for tumors with response scores 3-5, representing responders, and response scores 1-2, representing nonresponders. * indicates statistical significance ($P < .05$) and ** indicates statistical significance ($P < .001$).

comparing RS1-3 to RS4-5, and RS1-2 to RS3-5. Using RS5 as the cutoff (Figure 2A) for response yielded a significant difference in the percentage decrease between response groups as early as week 2 ($P < .05$); using RS4-5 as a cutoff (Figure 2B) required waiting until week 8 for a significant difference ($P < .05$) between response groups. Using RS3-5 as the cutoff (Figure 2C) for response resulted in no significant difference, although this is likely due to the limited sample size of the RS1-2 group ($n = 10$).

Discussion and Conclusion

This study evaluated tumor strain as a measure of NAC response in 92 locally advanced breast cancer patients. The images obtained were consistent with previous studies of locally advanced breast cancer [23] and appeared noisier than typical correlational elastography images from studies of much smaller breast masses. These patients have large

Table 2. Summary of Statistical Measures and Results.

	Decrease in SR from Baseline (% ± SD)	
	pCR: RS5 ($n = 21$)	Non-pCR: RS1-4 ($n = 71$)
Week 1	4 ± 13	-1 ± 9
Week 2	12 ± 13*	3 ± 11*
Week 4	19 ± 13**	6 ± 11**
Week 8	25 ± 16**	9 ± 11**
Week 12	30 ± 17**	14 ± 13**
Preoperative	29 ± 15**	12 ± 13**

	Decrease in SR from Baseline (% ± SD)	
	RS4-5 ($n = 37$)	RS1-3 ($n = 39$)
Week 1	3 ± 11	-1 ± 9
Week 2	7 ± 13	2 ± 9
Week 4	11 ± 15	6 ± 10
Week 8	17 ± 16*	9 ± 11*
Week 12	21 ± 18*	14 ± 13*
Preoperative	20 ± 16*	13 ± 13*

	Decrease in SR from Baseline (% ± SD)	
	RS3-5 ($n = 66$)	RS1-2 ($n = 10$)
Week 1	0 ± 10	0 ± 7
Week 2	5 ± 12	1 ± 8
Week 4	9 ± 13	4 ± 10
Week 8	14 ± 15	7 ± 10
Week 12	18 ± 15	15 ± 23
Preoperative	17 ± 15	12 ± 14

SRs for each response group, as categorized by the indicated Miller-Payne criteria, were analyzed for statistical differences over time using a repeated-measures ANOVA. Responders and nonresponders were compared to each other at each time interval to test for statistically significant differences following a test for normality (Shapiro-Wilk Test). Statistically significant, $*P < .05$; very statistically significant, $**P < .001$.

locally advanced tumors, and their breasts are often grossly enlarged and taut to the touch. These tumors have a great deal of associated edema, and inflammation of the whole breast is often apparent clinically. The breasts are often clinically “rock hard,” “red,” and “hot” to the touch. This also makes elastography imaging more difficult with the tumor tissue being not that different from the surrounding tissue in terms of stiffness. Unlike in classic strain imaging of small tumors, where tumors are readily identifiable, the masses here are very large (over 5 cm and typically 10-15 cm in longest diameter) and may occupy over 60% of the field of view. Overall, this results in differences between nonmalignant and malignant breast tissue being less evident in elastographic images despite apparent differences in the B-mode images.

Both the pCR and npCR patient groups demonstrated a significant change in tumor stiffness, with a decrease in stiffness from baseline

Table 3. ROC Analysis of SRs at Weeks 1, 4, and 8 and Preop.

	Naive Bayes Classification of pCR Versus Non-pCR			
	Week 1	Week 4	Week 8	Preoperatively
Accuracy	72 ± 5	84 ± 4	83 ± 4	84 ± 4
Sensitivity (%)	80	85	87	84
Specificity (%)	64	83	80	85
AUC	0.64	0.75	0.77	0.81

	k-NN Model Classification of pCR Versus Non-pCR			
	Week 1	Week 4	Week 8	Preoperatively
Accuracy	60 ± 3	73 ± 5	74 ± 3	72 ± 4
Sensitivity (%)	84	81	95	85
Specificity (%)	36	65	54	55
AUC	0.44	0.72	0.66	0.64

Sensitivity (%Sn), specificity (%Sp), accuracy (%), and AUCs are presented for SRs corresponding to the measured time intervals.

apparent by weeks 2 ($P < .05$) and 4 ($P < .001$). The SR decrease from baseline was significantly different between the two groups by week 2 ($P < .01$). Using alternative definitions of responsiveness, RS4-5 and RS3-5 classifications instead of pCR (RS5), was not as effective in differentiating the two groups, with the former only achieving a significant difference between response groups by week 8 and the latter not achieving any significant difference (although this is likely a result of limited sample size). Preoperatively, data indicated that measures of tumor stiffness achieved a classification of pCR and npCR with a sensitivity of 84%, a specificity of 85%, and AUC of 81%.

The results of this study suggest that changes in tumor stiffness in response to NAC can be used as an early-response marker during treatment, with significant results detected by week 2 of treatment and the best results obtained preoperatively. Preoperative elastography data would likely have minimal effect on guiding further treatment and little benefit aside from potentially being used as a confirmatory test. However, being able to assess NAC response as early as 2 weeks into treatment could be beneficial for treatment planning, as ineffective chemotherapy regimens could be halted and new therapeutic options pursued. Changing the course of treatment for a nonresponding patient would spare them the adverse effects associated with the ineffective chemotherapy while offering the possibility of an improved outcome by switching to a more effective therapy earlier.

Characterizing a tumor's mechanical properties enables the response to NAC to be assessed even when it may not be visually apparent using traditional anatomical imaging methods. Cancerous tissues have complex mechanical properties. Here we have made the simplifying assumption that the tissue is linearly elastic and isotropic, which is not always the case for tumors. This assumption may result in strain values that are not entirely accurate. However, we are particularly interested in evaluating changes in the relative stiffness in the same tissues before and after treatment rather than the actual strain values measured. Stiffness in tumor extracellular matrix has been associated with increased progression and chemotherapeutic resistance in breast lesions and in other types of malignancies [28–30]. A prior study by Hayashi et al. found greater rates of pathologically complete response to NAC among tumors with lower stiffness as categorized by the Tsukuba elasticity scoring system [31]. Ultrasound elastography, as an imaging modality, has already been shown to be effective in characterizing breast lesions. Most notably, it can be used in combination with B-mode ultrasound to differentiate between malignant and benign lesions [32,33]. Shear-wave ultrasound, another ultrasound-based modality which characterizes tissue stiffness, has been used to establish a relationship between stiffness and the histological grade and molecular subtype of breast lesions [34–36]. Several studies have relied on the SR, as defined in the study here to characterize breast lesions [23,27,37–40]. We demonstrated that changes in the SR correlate with tumor response to treatment.

We performed a subanalysis (Supplementary Figure 1, Supplementary Table 1) and found no difference between luminal, basal, and HER-2-enriched groups. It was difficult to conclude at which week during treatment the absolute SR value was significantly different from the initial SR baseline value. Luminal cancers exhibited changes as early as week 1, whereas basal cancers exhibited changes in SR at week 8 only. How early a change was apparent seemed to be more dependent on the sample size of the study rather than the magnitude of the change. The HER-2-enriched group saw no

significant decrease from baseline in either the pCR group or npCR group, most likely due to a small sample size ($n = 5$ for each). Additionally, a lack of access to Ki-67 data limited the degree to which tumors could be classified. For example, luminal A and luminal B subtypes could not be distinguished from each other and had to be grouped together.

A study by Falou et al. which examined a smaller patient population of 13 indicated a change in stiffness in tumors that responded to NAC. However, contrary to our study, there was no significant change in the SR in nonresponding tumors [23]. The difference seen in the study here can likely be attributed to the larger patient population examined or to the fact that the other work compared patients using a broad definition of nonresponders to responders, whereas this study compares pCR to npCR. The study by Falou et al. also demonstrated that the SR was superior to the strain difference with respect to evaluating response to NAC via elastography. For that reason, SR was chosen as the variable used in our analysis. Pathological complete response (RS5) was chosen as the basis of comparison rather than overall response (RS3-5) because it is a better indicator of overall clinical outcome [8]. The predictive power of compression elastography is limited in that both npCR and pCR response groups experience a decrease in SR in response to NAC — it is only the magnitude of that change which differs. With that said, it is important to consider that the npCR response group contains partial responders. Partial response is still important as it is linked to good outcomes among certain subtypes, and it may enable patients to have achieved sufficient downstaging to sanction breast-conserving surgery as a treatment option, [8]. Other studies have found a benefit in combining other measures of tumor response with elastography data to improve its predictive power, such as Ki-67 indices [41].

Unlike previous studies, which were able to establish a relationship between tumor stiffness and molecular subtype using shear-wave elastography [35], no significant differences between molecular subtypes were seen in this study. This may be explained by the low power that resulted from only 10 HER-2-enriched tumors being examined. Obtaining significant results at low sample sizes is challenging using this imaging modality due to a large degree of interpatient variability in SR measurements.

An imaging modality capable of assessing tumor response to NAC early in the course of treatment could help optimize therapy in cases where NAC is ineffective. A systematic review by Gu et al. stated that diffusion-weighted MRI and contrast-enhanced MRI combined with PET/CT were both superior modalities compared to standard ultrasonography in the detection of pCR [32,42]. However, ultrasound still has the advantage of being more accessible for use at frequent intervals during the course of NAC. Throughout our study, most patients were scanned at six time intervals following the baseline scan, with a significant difference seen between pCR and npCR groups by week 2. The use of compression elastography permits accessible noninvasive imaging, which is sensitive to biomolecular changes that may occur prior to anatomical changes seen in tumors by clinical imaging. Prior studies have shown quantitative ultrasound to also have the potential to evaluate response to NAC [22,43], with further promising results seen when used in conjunction with other modalities such as diffuse optical spectroscopy [44]. Future studies could involve using elastography as part of a multiparametric analysis of tumor response in addition to quantitative ultrasound.

Although strain ultrasound would be a practical and resource-efficient imaging modality to monitor response to NAC, there are various limitations to its implementation in clinical practice. Strain ultrasound involves the operator applying a manual compression force via the transducer. Although the ultrasound apparatus determines that adequate compression is applied between scans, this practice is nonquantitative and has an inherent lack of consistency and reproducibility. Freehand elastography, in which the tissue compression is generated by hand via the ultrasound transducer, has the main advantage of being practical in a clinical setting. Since elastography images are generated by comparing the axial displacement of the tissue before and after compression, any out-of-plane motion will result in reduced signal to noise ratio (SNR) [45]. Mechanical attachments to the transducer, such as compression applicators, can significantly reduce out-of-plane motion; however, they require additional hardware and make the imaging transducer more bulky and difficult to handle. The native software of the Ultrasonix system uses a least squares strain estimator to improve SNR [46]. This method does not directly correct for the interframe decorrelation caused by out-of-plane motion. Several methods to correct for this type of motion have been investigated including guiding data acquisition through real-time feedback [47] as well as postprocessing algorithms [48,49]. The implementation of such methods could provide some improvement in the SNR and consistency of the strain images.

In conclusion, the magnitude of a tumor's change in stiffness in response to NAC may be used as a predictor of pathologically complete response. Compression elastography is a readily available imaging modality; therefore, improving its utility in the clinical setting would be highly beneficial. Real-time monitoring of tumor response to NAC has the potential to spare unresponsive patients from prolonged unsuccessful treatment regimens. Compression ultrasound should be further investigated as it shows potential to serve as an imaging modality that would achieve this in a practical setting.

Supplementary data to this article can be found online at <https://doi.org/10.1016/j.tranon.2019.05.004>.

Author Contributions

Jason Fernandes: data analysis, data curation, manuscript writing

William T. Tran: manuscript review and editing, methodology, supervision, data

collection, data curation

Alexander Koven: data collection

Elyse Watkins: data collection, data curation

Farnoosh Hadizad: data collection

Sonal Gandhi: data collection

Frances Wright: data collection

Belinda Curpen: data collection

Ahmed El Kaffas: data collection

Joanna Falryn: data collection

Ali Sadeghi-Naini: data collection

Gregory Czarnota: conceptualization, review and editing of manuscript, data acquisition, methodology, supervision.

Funding

This study was funded by the Terry Fox Foundation, the Natural Sciences and Engineering Research Council (NSERC) of Canada, and the Federal Economic Development Agency for Southern Ontario (FedDev Ontario). Dr. Gregory J. Czarnota is supported

by a James and Mary Davie Chair in Breast Cancer Imaging and Ablation at the University of Toronto.

References

- [1] Canadian Cancer Society's Advisory Committee on Cancer Statistics. Canadian cancer statistics (2016). Canadian Cancer Statistics. Toronto: ON; 2016 2016.
- [2] BC Cancer Agency. 6.5 Locally advanced breast cancer (T3N1; Any T4; Any N2N3M0) [Internet]. Available from <http://www.bccancer.bc.ca/books/breast/management/inflammatory-breast-cancer>
- [3] Garg PK and Prakash G (2015). Current definition of locally advanced breast cancer. *Curr Oncol* . <http://dx.doi.org/10.3747/co.22.2697>.
- [4] Gradishar WJ, Anderson BO, Balassanian R, Blair SL, Burstein HJ, Cyr A, Elias AD, Farrar WB, Forero A, Giordano SH, Goetz M, Goldstein LJ, Hudis CA, et al. NCCN clinical practice guidelines in oncology: breast cancer version 2.2015. *J Natl Compr Cancer Netw* [Internet]. 2015; 13: 448–75. doi: 10.6004/jncn.2015.0060.
- [5] Tryfonidis K, Senkus E, Cardoso MJ, and Cardoso F (2015). Management of locally advanced breast cancer-perspectives and future directions. *Nat Rev Clin Oncol* 12, 147–162. <http://dx.doi.org/10.1038/nrclinonc.2015.13> Internet.
- [6] Brackstone M, Fletcher GG, Dayes IS, Madarnas Y, SenGupta SK, and Verma S (2014). Disease Site Group M of the BC. Locoregional therapy of locally advanced breast cancer: a clinical practice guideline. *Curr Oncol [Internet]* 22, 54. <http://dx.doi.org/10.3747/co.22.2316>.
- [7] Marchiò C and Sapino A (2011). The pathologic complete response open question in primary therapy. *J Natl Cancer Inst - Monogr* . <http://dx.doi.org/10.1093/jncimonographs/lgr025>.
- [8] von Minckwitz G, Untch M, Blohmer J-U, Costa SD, Eidtmann H, Fasching PA, Gerber B, Eiermann W, Hilfrich J, and Huober J, et al (2012). Definition and impact of pathologic complete response on prognosis after neoadjuvant chemotherapy in various intrinsic breast cancer subtypes. *J Clin Oncol* 30, 1796–1804. <http://dx.doi.org/10.1200/JCO.2011.38.8595> Internet.
- [9] Galow JR, Burstein HJ, Wood W, Hortobagyi GN, Gianni L, von Minckwitz G, Buzdar AU, Smith IE, Symmans WF, and Singh B, et al (2008). Preoperative therapy in invasive breast cancer: pathologic assessment and systemic therapy issues in operable disease. *J Clin Oncol* 26, 814–819. <http://dx.doi.org/10.1200/JCO.2007.15.3510> Internet.
- [10] Belli P, Costantini M, Malaspina C, Magistrelli A, LaTorre G, and Bonomo L (2006). MRI accuracy in residual disease evaluation in breast cancer patients treated with neoadjuvant chemotherapy. *Clin Radiol* 61, 946–953. <http://dx.doi.org/10.1016/j.crad.2006.07.004> Internet.
- [11] Tiling R, Linke R, Untch M, Richter A, Fieber S, Brinkbäumer K, Tatsch K, and Hahn K (2001). 18F-FDG PET and 99mTc-sestamibi scintimammography for monitoring breast cancer response to neoadjuvant chemotherapy: a comparative study. *Eur J Nucl Med* . <http://dx.doi.org/10.1007/s002590100539>.
- [12] Groheux D, Hindié E, Giacchetti S, Delord M, Hamy A-S, de Roquancourt A, Vercellino L, Berenger N, Marty M, and Espié M (2012). Triple-negative breast cancer: early assessment with 18F-FDG PET/CT during neoadjuvant chemotherapy identifies patients who are unlikely to achieve a pathologic complete response and are at a high risk of early relapse. *J Nucl Med* 53, 249–254. <http://dx.doi.org/10.2967/jnumed.111.094045> Internet.
- [13] Wang Y, Zhang C, Liu J, and Huang G (2012). Is 18F-FDG PET accurate to predict neoadjuvant therapy response in breast cancer? A meta-analysis. *Breast Cancer Res Treat* . <http://dx.doi.org/10.1007/s10549-011-1780-z>.
- [14] Chagpar AB, Middleton LP, Sahin AA, Dempsey P, Buzdar AU, Mirza AN, Ames FC, Babiera GV, Feig BW, and Hunt KK, et al (2006). Accuracy of physical examination, ultrasonography, and mammography in predicting residual pathologic tumor size in patients treated with neoadjuvant chemotherapy. *Ann Surg* 243, 257–264. <http://dx.doi.org/10.1097/01.sla.0000197714.14318.6f> Internet.
- [15] Evans A, Armstrong S, Whelehan P, Thomson K, Rauchhaus P, Purdie C, Jordan L, Jones L, Thompson A, and Vinnicombe S (2013). Can shear-wave elastography predict response to neoadjuvant chemotherapy in women with invasive breast cancer? *Br J Cancer* 109, 2798–2802. <http://dx.doi.org/10.1038/bjc.2013.660> Internet.
- [16] Gennisson J-L, Deffieux T, Fink M, and Tanter M (2013). Ultrasound elastography: principles and techniques. *Diagn Interv Imaging* 94, 487–495. <http://dx.doi.org/10.1016/j.diii.2013.01.022> Internet.
- [17] Sigrist RMS, Liao J, El Kaffas A, Chammam MC, and Willmann JK (2017). Ultrasound elastography: review of techniques and clinical applications. *Theranostics* 7, 1303–1329. <http://dx.doi.org/10.7150/thno.18650> Internet.

- [18] Junker D, De Zordo T, Quentin M, Ladurner M, Bektic J, Horniger W, Janschke W, Aigner F. Real-time elastography of the prostate. *Biomed Res Int* [Internet]. 2014; 2014: 180804. doi: <https://doi.org/10.1155/2014/180804>.
- [19] Faruk T, Islam MK, Arefin S, and Haq MZ (2015). The journey of elastography: background, current status, and future possibilities in breast cancer diagnosis. *Clin Breast Cancer* **15**, 313–324. <http://dx.doi.org/10.1016/j.clbc.2015.01.002> Internet.
- [20] Sun J, Cai J, and Wang X (2014). Real-time ultrasound elastography for differentiation of benign and malignant thyroid nodules: a meta-analysis. *J Ultrasound Med* **33**, 495–502. <http://dx.doi.org/10.7863/ultra.33.3.495> Internet.
- [21] Chang JM, Won J-K, Lee K-B, Park IA, Yi A, and Moon WK (2013). Comparison of shear-wave and strain ultrasound elastography in the differentiation of benign and malignant breast lesions. *AJR Am J Roentgenol* **201**, W347–W356. <http://dx.doi.org/10.2214/AJR.12.10416> Internet.
- [22] Sadeghi-Naini A, Papanicolaou N, Falou O, Zubovits J, Dent R, Verma S, Trudeau M, Boileau JF, Spayne J, Iradji S, Sofroni E, Lee J, Lemon-Wong S, et al. Quantitative ultrasound evaluation of tumor cell death response in locally advanced breast cancer patients receiving chemotherapy. *Clin Cancer Res* [Internet]. 2013; 19: 2163–74. Available from <http://clincancerres.aacrjournals.org/cgi/doi/10.1158/1078-0432.CCR-12-2965>
- [23] Falou O, Sadeghi-Naini A, Prematilake S, Sofroni E, Papanicolaou N, Iradji S, Jahedmotlagh Z, Lemon-Wong S, Pignol J-P, and Rakovitch E, et al (2013). Evaluation of neoadjuvant chemotherapy response in women with locally advanced breast cancer using ultrasound elastography. *Transl Oncol* **6**, 17–24. <http://dx.doi.org/10.1593/tlo.12412> Internet.
- [24] Ophir J, Alam SK, Garra BS, Kallel F, Konofagou EE, Krouskop T, Merritt CRB, Righetti R, Souchon R, and Srinivasan S, et al (2002). Elastography: imaging the elastic properties of soft tissues with ultrasound. *J Med Ultrason* **29**, 155–171. <http://dx.doi.org/10.1007/BF02480847> Internet.
- [25] Zahiri-Azar R and Salcudean SE (2006). P1A-3 real-time estimation of lateral displacement using time domain cross correlation with prior estimates. 2006 IEEE Ultrasonics Symposium [Internet]. *IEEE*, 1209–1212. <http://dx.doi.org/10.1109/ULTSYM.2006.309>.
- [26] Zhi H, Xiao X-Y, Yang H-Y, Ou B, Wen Y-L, and Luo B-M (2010). Ultrasonic elastography in breast cancer diagnosis: strain ratio vs 5-point scale. *Acad Radiol [Internet]* **17**, 1227–1233. <http://dx.doi.org/10.1016/j.acra.2010.05.004>.
- [27] Nesje L, Havre R, Waage J, Mulabecirovic A, and Gilja O (2018). Strain ratio as a quantification tool in strain imaging. *Appl Sci* **8**, 1273. <http://dx.doi.org/10.3390/app8081273>.
- [28] Ulrich TA, de Juan Pardo EM, and Kumar S (2009). The mechanical rigidity of the extracellular matrix regulates the structure, motility, and proliferation of glioma cells. *Cancer Res* **69**, 4167–4174. <http://dx.doi.org/10.1158/0008-5472.CAN-08-4859> Internet.
- [29] Levental KR, Yu H, Kass L, Lakins JN, Egeblad M, Erler JT, Fong SFT, Csiszar K, Giaccia A, and Weninger W, et al (2009). Matrix crosslinking forces tumor progression by enhancing integrin signaling. *Cell* **139**, 891–906. <http://dx.doi.org/10.1016/j.cell.2009.10.027> Internet.
- [30] Schrader J, Gordon-Walker TT, Aucott RL, van Deemter M, Quaas A, Walsh S, Benten D, Forbes SJ, Wells RG, and Iredale JP (2011). Matrix stiffness modulates proliferation, chemotherapeutic response, and dormancy in hepatocellular carcinoma cells. *Hepatology*. <http://dx.doi.org/10.1002/hep.24108>.
- [31] Hayashi M, Yamamoto Y, Ibusuki M, Fujiwara S, Yamamoto S, Tomita S, Nakano M, Murakami K, Iyama K-I, and Iwase H (2012). Evaluation of tumor stiffness by elastography is predictive for pathologic complete response to neoadjuvant chemotherapy in patients with breast cancer. *Ann Surg Oncol* **19**, 3042–3049. <http://dx.doi.org/10.1245/s10434-012-2343-1> Internet.
- [32] Chung J, Lee WK, Cha E-S, Lee JE, Kim JH, Ryu YH. Shear-wave elastography for the differential diagnosis of breast papillary lesions. *PLoS One* [Internet]. 2016; 11: e0167118. doi: <https://doi.org/10.1371/journal.pone.0167118>.
- [33] Bayar M, Denis M, Gregory A, Mehromohammadi M, Kumar V, Meixner D, Fazzio RT, Fatemi M, and Alizad A (2017). Diagnostic features of quantitative comb-push shear elastography for breast lesion differentiation. *PLoS One*. <http://dx.doi.org/10.1371/journal.pone.0172801>.
- [34] Denis M, Gregory A, Bayar M, Fazzio RT, Whaley DH, Ghosh K, Shah S, Fatemi M, Alizad A. Correlating tumor stiffness with immunohistochemical subtypes of breast cancers: prognostic value of comb-push ultrasound shear elastography for differentiating luminal subtypes. *PLoS One* [Internet]. 2016; 11: e0165003. doi: <https://doi.org/10.1371/journal.pone.0165003>.
- [35] Chang JM, Park IA, Lee SH, Kim WH, Bae MS, Koo HR, Yi A, Kim SJ, Cho N, and Moon WK (2013). Stiffness of tumours measured by shear-wave elastography correlated with subtypes of breast cancer. *Eur Radiol* **23**, 2450–2458. <http://dx.doi.org/10.1007/s00330-013-2866-2> Internet.
- [36] Choi WJ, Kim HH, Cha JH, Shin HJ, Kim H, Chae EY, and Hong MJ (2014). Predicting prognostic factors of breast cancer using shear wave elastography. *Ultrasound Med Biol* **40**, 269–274. <http://dx.doi.org/10.1016/j.ultrasmed-bio.2013.09.028> Internet.
- [37] Shin JK. The breast tumor strain ratio is a predictive parameter for axillary lymph node metastasis in patients with invasive breast cancer. 2015; : 630–8. doi: <https://doi.org/10.2214/AJR.14.14269>.
- [38] Stoian D, Timar B, Craina M, Bernad E, and Petre I (2016). Qualitative strain elastography — strain ratio evaluation — an important tool in breast cancer diagnostic. *Med Ultrason* **18**, 195–200. <http://dx.doi.org/10.11152/mu.2013.2066.182.bcd>.
- [39] Ikora MIS, Ida KR V, Acovski MIP, Timac DAS. Implementation of elastography score and strain ratio in combination with B-mode ultrasound avoids unnecessary biopsies of breast lesions. 2017; 43: 804–16. doi: <https://doi.org/10.1016/j.ultrasmedbio.2016.11.019>.
- [40] Ricci P, Maggini E, Mancuso E, Lodise P, Cantisani V, and Catalano C (2013). Clinical application of breast elastography: state of the art; 2013 1–9.
- [41] Ma Y, Zhang S, Zang L, Li J, Li J, Kang Y, and Ren W (2016). Combination of shear wave elastography and Ki-67 index as a novel predictive modality for the pathological response to neoadjuvant chemotherapy in patients with invasive breast cancer. *Eur J Cancer* **69**, 86–101. <http://dx.doi.org/10.1016/j.ejca.2016.09.031> Internet.
- [42] Gu Y-L, Pan S-M, Ren J, Yang Z-X, and Jiang G-Q (2017). Role of magnetic resonance imaging in detection of pathologic complete remission in breast cancer patients treated with neoadjuvant chemotherapy: a meta-analysis. *Clin Breast Cancer*. <http://dx.doi.org/10.1016/j.clbc.2016.12.010>.
- [43] Tadayyon H, Sannachi L, Gangeh M, Sadeghi-Naini A, Tran W, Trudeau ME, Pritchard K, Ghandi S, Verma S, and Czarnota GJ (2016). Quantitative ultrasound assessment of breast tumor response to chemotherapy using a multi-parameter approach. *Oncotarget*. <http://dx.doi.org/10.18632/oncotarget.8862>.
- [44] Falou O, Soliman H, Sadeghi-Naini A, Iradji S, Lemon-Wong S, Zubovits J, Spayne J, Dent R, Trudeau M, and Boileau JF, et al (2012). Diffuse optical spectroscopy evaluation of treatment response in women with locally advanced breast cancer receiving neoadjuvant chemotherapy. *Transl Oncol* **5**, 238–246. <http://dx.doi.org/10.1593/tlo.11346> Internet.
- [45] Seelamantula CS, Villiger ML, Ra Leitgeb, and Unser M (2008). Exact and efficient signal reconstruction in frequency-domain optical-coherence tomography. *J Opt Soc Am A Opt Image Sci Vis* **25**, 1762–1771. <http://dx.doi.org/10.1364/JOSAA.25.001762>.
- [46] Kallel F and Ophir J (1997). A Least-squares strain estimator for elastography. *Ultrason Imaging* **19**, 195–208. <http://dx.doi.org/10.1177/016173469701900303> Internet.
- [47] Hall TJ, Zhu Y, and Spalding CS (2003). In vivo real-time freehand palpation imaging. *Ultrasound Med Biol* **29**, 427–435. [http://dx.doi.org/10.1016/S0301-5629\(02\)00733-0](http://dx.doi.org/10.1016/S0301-5629(02)00733-0) Internet.
- [48] Foroughi P, Kang H-J, Carnegie DA, van Vledder MG, Choti MA, Hager GD, and Boctor EM (2013). A Freehand ultrasound elastography system with tracking for in vivo applications. *Ultrasound Med Biol* **39**, 211–225. <http://dx.doi.org/10.1016/j.ultrasmedbio.2012.09.006> Internet.
- [49] Hiltawsky KM, Krüger M, Starke C, Heuser L, Ermert H, Jensen A. Freehand ultrasound elastography of breast lesions: clinical results. *Ultrasound Med Biol* [Internet]. 2001; 27: 1461–9. Available from <http://www.ncbi.nlm.nih.gov/pubmed/11750744>